Supporting Information

Photoactive Metal-Organic Framework as Bifunctional Materials for 4-Hydroxy-4'-nitrobiphenyl Detection and Photodegradation of Methylene Blue

Lingling Xia,[a] Jiawen Ni,[a] Pengyan Wu,[a]* Ju Ma,[a] Liang Bao,[a] Yanhui Shi[a] and Jian Wang[a]*

[a]School of Chemistry and Materials Science & Jiangsu Key Laboratory of Green Synthetic Chemistry for Functional Materials, Jiangsu Normal University, Xuzhou, 221116, P. R. China.

1. Experimental

Materials and Instrumentation: All reagents and solvents were of AR grade and used without further purification unless otherwise noted. 4,4',4"-tricarboxyltriphenylamine (H_3tca) was synthesised from literature methods.[S1] $Cd(NO_3)_2 \cdot 4H_2O$ and methylene blue were purchased from J&K Scientific, nitroaromatics were provided from Xiya Reagent Company (China). The high concentration stock solutions of related nitro-analysts (2.0×10^{-2} M) were prepared directly in ethanol solvents. X-Ray powder diffraction (XRD) patterns of the Cd−TCAA was recorded on a Rigaku D/max-2400 X−ray powder diffractometer (Japan) using Cu-*K*α (λ =1.5405 Å) radiation. Elemental analyses (C, H, N) were performed on an Elementar Vario EL analyzer. The Cd^{2+} contents before and after catalysis were measured by Inductively Coupled Plasma Spectrometer (Perkin Elmer). FT−IR spectra were recorded as KBr pellets on JASCO FT/IR−430. Fluorescence spectra of the solution were obtained using the F−4600 spectrometer (Hitachi). Solid Uv-vis spectra were recorded on a HP 8453 spectrometer. Uv-*vis* spectra were measured on a JASCO V-530 spectrometer. N_2 sorption isotherms were measured using a Micromeritics ASAP 2020 surface area analyzer. Before the measurements, the samples were degassed under high vacuum (<0.01 Pa) at 120 °C for 10 h.

Crystallography: Intensities were collected on a Bruker SMART APEX CCD diffractometer with graphitemonochromated Mo-*K*α (λ = 0.71073 Å) using the SMART and SAINT programs. The structure was solved by direct methods and refined on F^2 by full-matrix least-squares methods with SHELXTL *version* 5.1. Non-hydrogen atoms of the ligand backbones were refined anisotropically. Hydrogen atoms within the ligand backbones were fixed geometrically at calculated positions and allowed to ride on the parent non-hydrogen atoms.

2. X-ray Crystallography (Single-crystal diffraction) and Characterizations.

2.1 Figure S1 The structure of an asymmetric unit in Cd−TCAA.

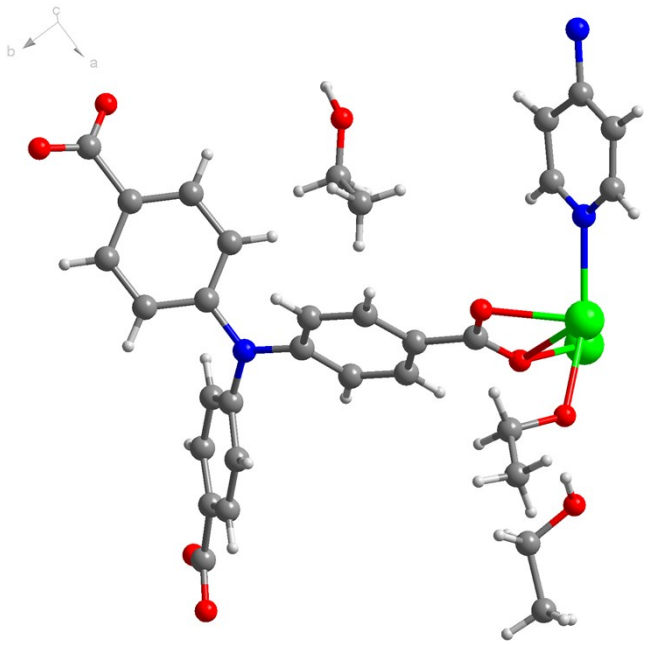

2.2 Selective bond distance (Å) and angle (°) in Cd−TCAA.

Selective bond distance(Å): Cd(1)-O(4A) 2.361(4)，Cd(1)-O(4B) 2.361(4), Cd(1)-O(1) 2.430(3), Cd(1)-O(1C) 2.430(3), Cd(1)-O(3B) 2.435(4), Cd(1)-O(3A) 2.435(4), Cd(1)-O(6D) 2.472(3), Cd(1)-O(6E) 2.472(3), Cd(2)-O(2) 2.323(3), Cd(2)-O(100) 2.320(4), Cd(2)-N(2) 2.347(4), Cd(2)-O(6D) 2.389(3), Cd(2)-O(5F) 2.396(4), Cd(2)-O(5D) 2.430(3), Cd(2)-O(1) 2.489(4).

Selective bond angle (°): O(4A)-Cd(1)-O(4B) 143.41(18), O(4A)-Cd(1)-O(1) 75.60(13), O(4B)-Cd(1)-O(1) 123.79(14), O(4A)-Cd(1)-O(1C) 123.79(14), O(4B)-Cd(1)-O(1C) 75.60(13), O(1)-Cd(1)-O(1C) 121.36(17), O(4A)-Cd(1)-O(3B) 146.51(14), O(4B)-Cd(1)-O(3B) 53.69(13), O(1)-Cd(1)-O(3B) 73.81(13), O(1)-Cd(1)-O(3) 84.36(13), O(4A)-Cd(1)-O(3A) 53.69(13), O(4B)-Cd(1)-O(3A) 146.51(14), O(1)-Cd(1)-O(3A) 84.36(13), O(1C)-Cd(1)-O(3A) 73.81(13), O(3B)-Cd(1)-O(3A) 134.70(19), O(4A)-Cd(1)-O(6D) 75.08(13), O(4B)-Cd(1)-O(6D) 79.27(12), O(1)-Cd(1)-O(6D) 77.99(11), O(1C)-Cd(1)-O(6D) 154.19(12), O(3B)-Cd(1)-O(6D) 85.49(12),O(3A)-Cd(1)-O(6D) 128.53(12), O(4A)-Cd(1)-O(6E) 79.27(12), O(4B)-Cd(1)-O(6E) 75.08(13), O(1)-Cd(1)-O(6E) 154.19(12), O(1C)-Cd(1)-O(6E) 77.99(11), O(3B)-Cd(1)-O(6E) 128.53(12), O(3A)-Cd(1)-O(6E) 85.49(12), O(6D)-Cd(1)-O(6E) 90.06(15), O(2)-Cd(2)-O(100) 85.81(17), O(2)-Cd(2)-N(2) 84.66(15), O(100)-Cd(2)-N(2) 150.3(2), O(2)-Cd(2)-O(6D) 122.91(12), O(100)-Cd(2)-O(6D) 116.28(18), O(100)-Cd(2)-O(2) 85.81(17), O(2)-Cd(2)-N(2) 84.66(15), O(100)-Cd(2)-O(6) 116.28(18), N(2)-Cd(2)-O(6) 92.34(14), O(2)-Cd(2)-O(6D) 122.91(12), O(100)-Cd(2)-O(6D) 116.39(17), N(2)-Cd(2)-O(6D) 92.34(14), O(2)-Cd(2)-O(5F) 116.95(13), O(100)-Cd(2)-O(5F) 79.21(17), N(2)-Cd(2)-O(5F) 80.27(15), O(6D)-Cd(2)-O(5F) 118.59(12), O(2)-Cd(2)-O(5D) 168.72(14), O(100)-Cd(2)-O(5D) 87.15(18), N(2)-Cd(2)-O(5D) 105.67(16), O(6D)-Cd(2)-O(5D) 53.40(12), O(5F)-Cd(2)-O(5D) 70.17(14), O(2)-Cd(2)-O(1) 53.88(12), O(100)-Cd(2)-O(1) 78.61(15), N(2)-Cd(2)-O(1) 116.93(14), O(6D)-Cd(2)-O(1) 78.43(11), O(5F)-Cd(2)-O(1) 156.58(13), O(5D)-Cd(2)-O(1) 115.97(12).

Symmetry codes: A. 0.5+x, -0.5+y, z; B. -0.5-x, -0.5+y, 0.5-z; C. -x, y, 0.5-z; D. -x, -1+y, z; E. x, -1+y, z; F. x, 2-y, -0.5+z.

2.3 Figure S2 PXRD patterns of the as-synthesized (red), the simulated from single X-ray crystal structure (black).

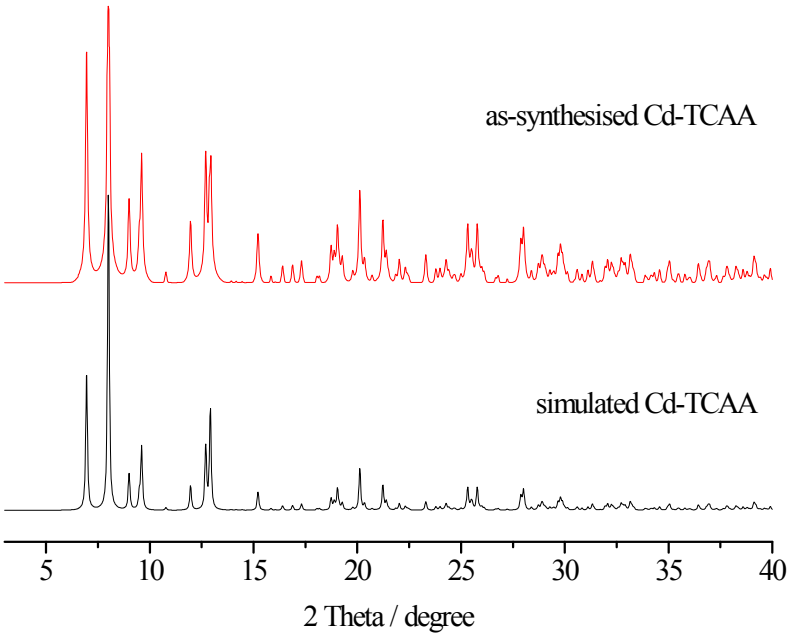

2.4 Figure S3 N_2 sorption isotherms of Cd−TCAA and Cd−TCAA after 5 cycles photodegradation of MB at 77 K.

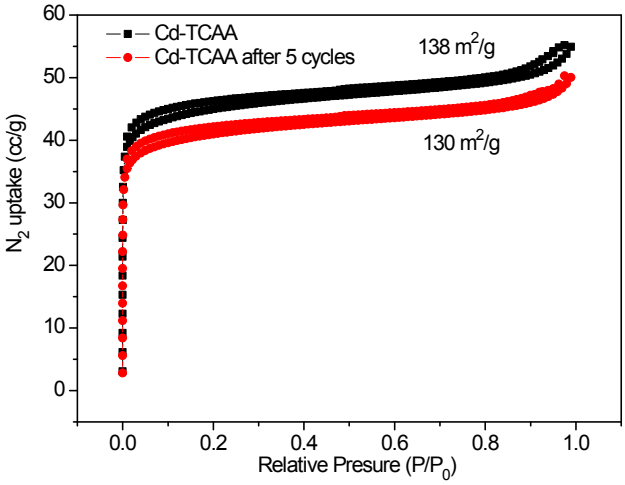

2.5 Figure S4 NLDFT pore size distribution of Cd−TCAA and Cd−TCAA after 5 cycles photodegradation of MB.

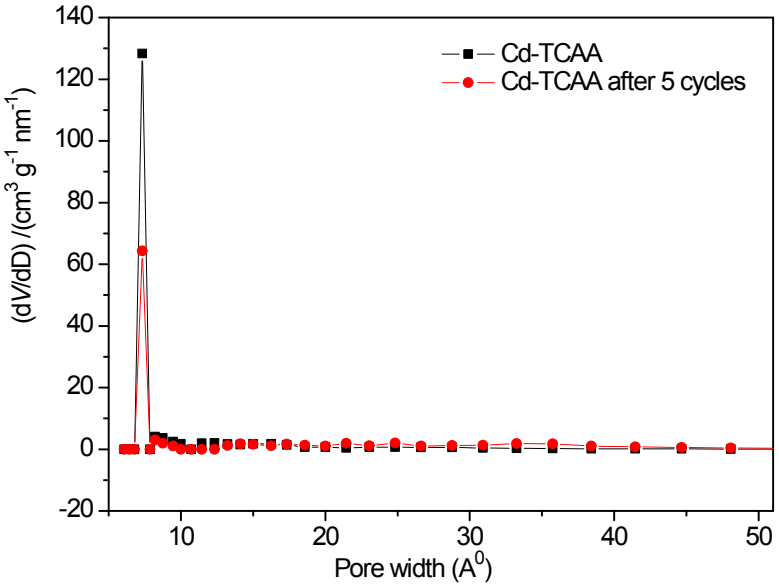

2.6 Figure S5 TGA profile of Cd−TCAA and activatedCd−TCAA in air.

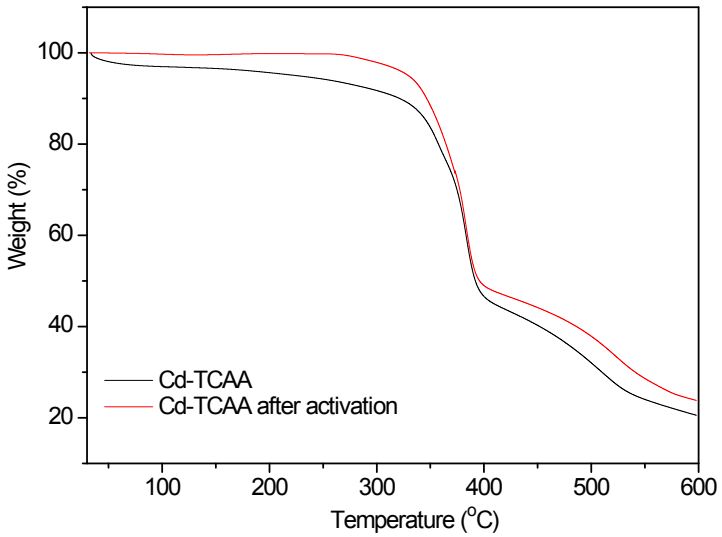

2.7 Table S1 The elemental analysis of Cd−TCAA after treated under different conditions, respectively. (The C/H/N were performed on an Elementar Vario EL analyser, the Cd^{2+} contents were measured by Inductively Coupled Plasma Spectrometer (Perkin Elmer))

	C(%)	**H(%)**	**N(%)**	**Cd(mM)**
Original Cd−TCAA (theoretical)	49.17	2.54	6.62	0.79
Original Cd−TCAA (found)	49.18	2.55	6.60	0.78
Treated under pH=2.5	49.19	2.55	6.61	0.77
Treated under pH=12.2	49.21	2.54	6.62	0.78

3. Studies on the nitro-explosives detection based on Cd−TCAA.

3.1 Figure S6 The UV/vis absorption spectra for solid Cd−TCAA.

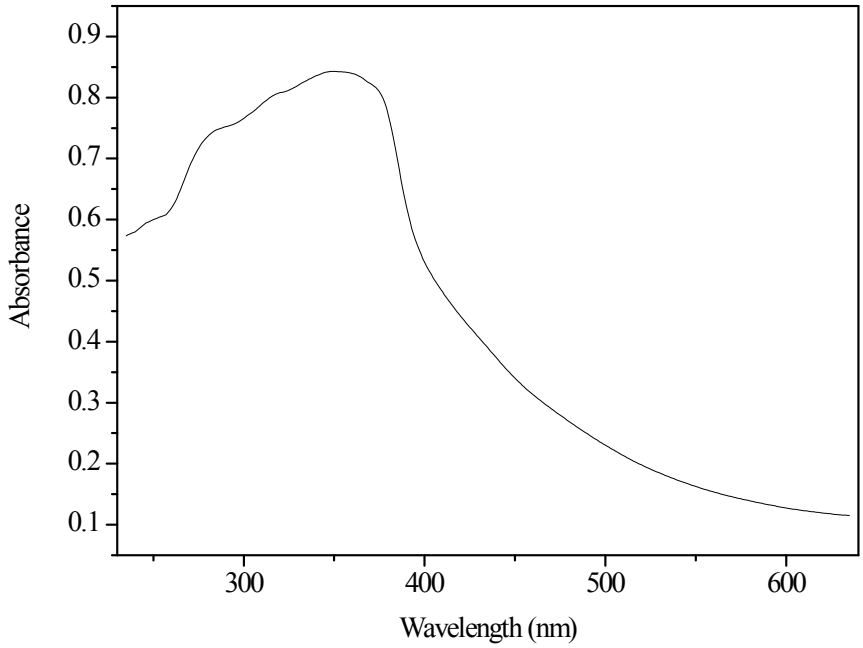

3.2 Figure S7 The Stern−Volmer plot of Cd−TCAA quenched by HNBP ethanol solution, where I_0 and I are the fluorescence intensity before and after HNBP incorporation, respectively.

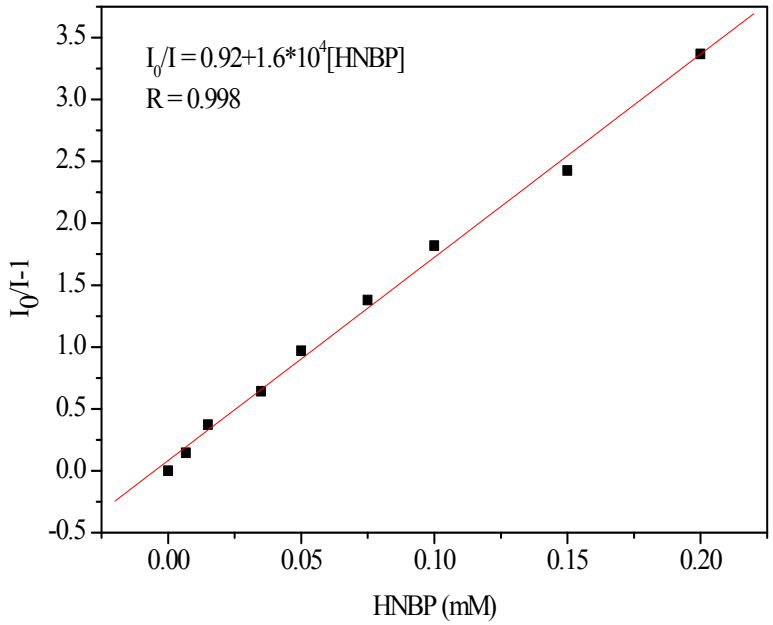

3.3 Figure S8 Families of various fluorescence spectra of Cd−TCAA (0.23 mM) in ethanol solution upon the addition of 0.3 mM of different selected analytes.

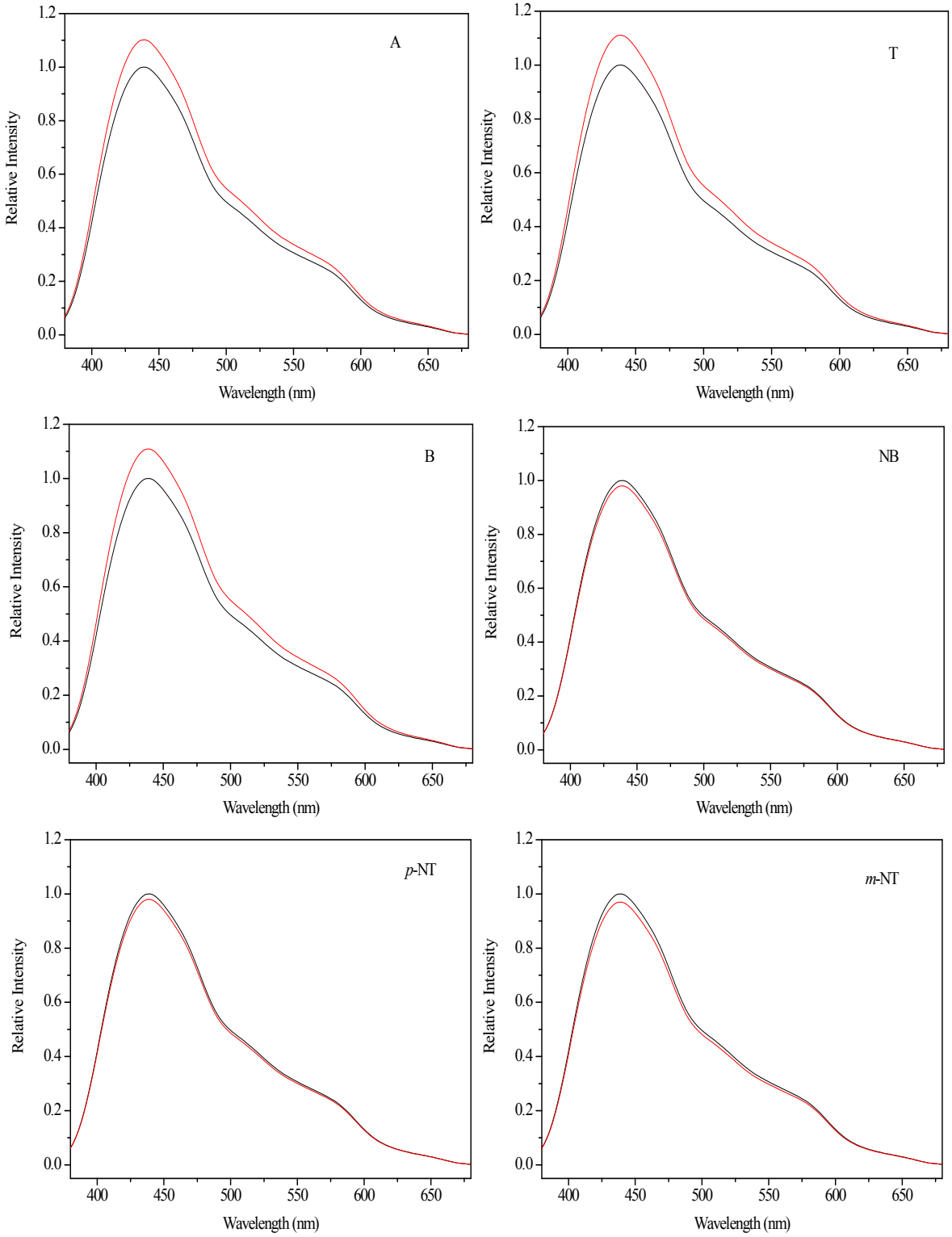

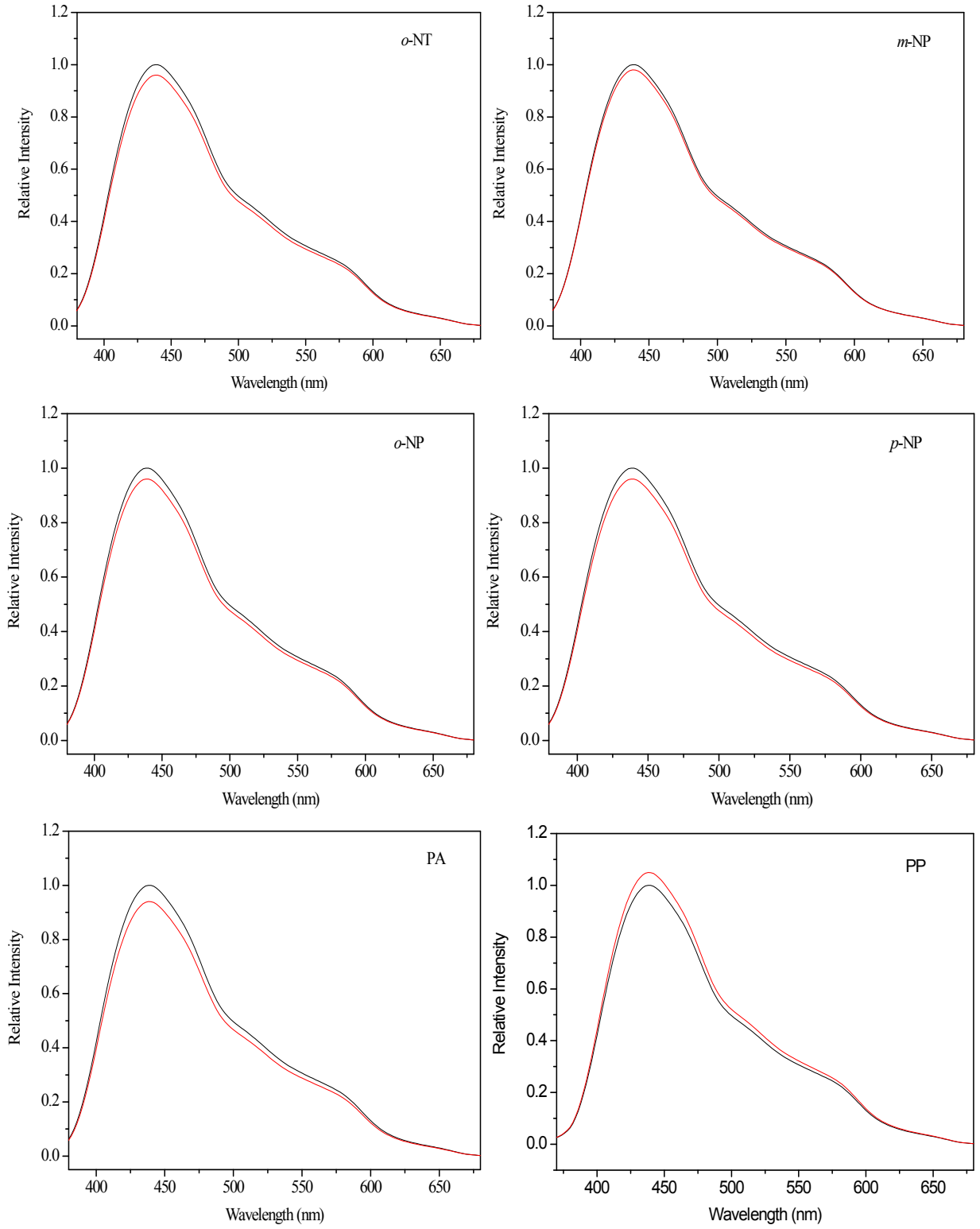
o-NT
m-NP
o-NP
p-NP
PA
PP
Relative Intensity
Wavelength (nm)
0.0
0.2
0.4
0.6
0.8
1.0
1.2
400
450
500
550
600
650

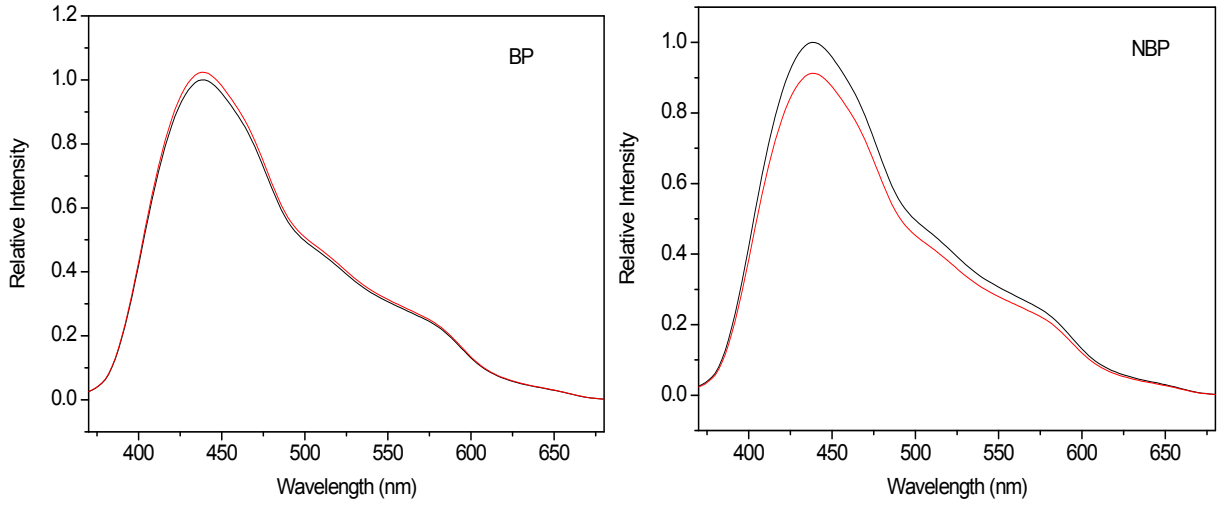

3.4 Figure S9 Family of fluorescence spectra of H_3tca in ethanol suspension upon the addition of 0.3 mM of HNBP.

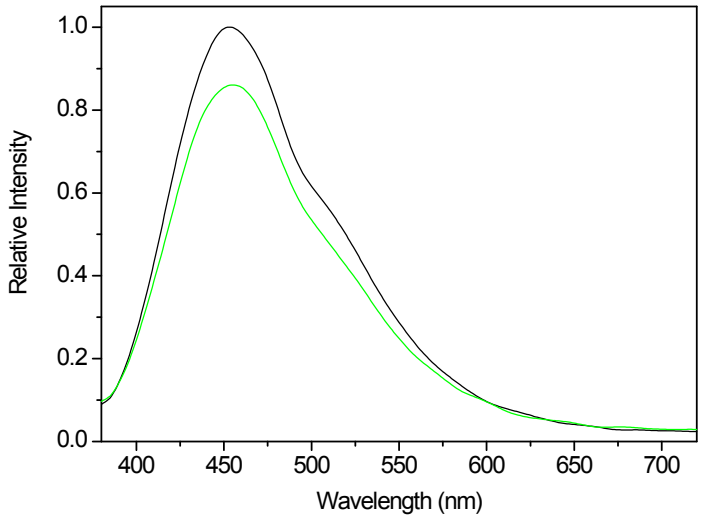

4. Studies on the photodegradation of MB based on Cd−TCAA.

4.1 Figure S10 The first-order plots for the photodegradation of MB using Cd−TCAA.

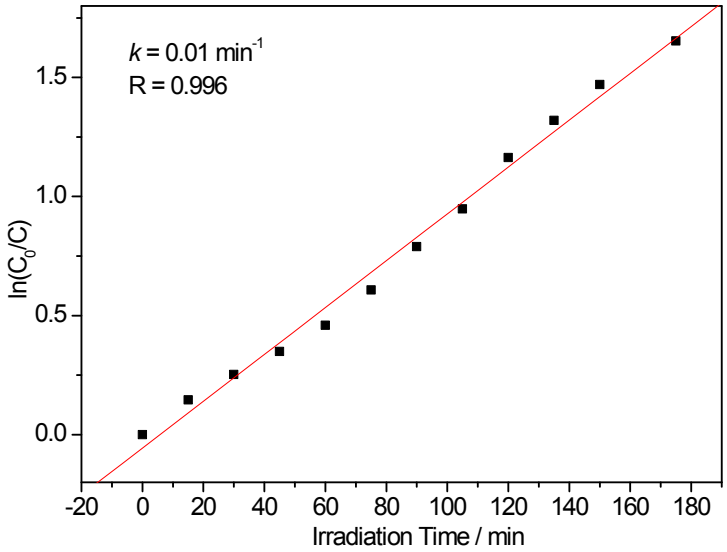

4.2 Figure S11 Powder XRD patterns of as-synthesized Cd−TCAA (black line), Cd−TCAA after 5 photocatalytic cycles (red line).

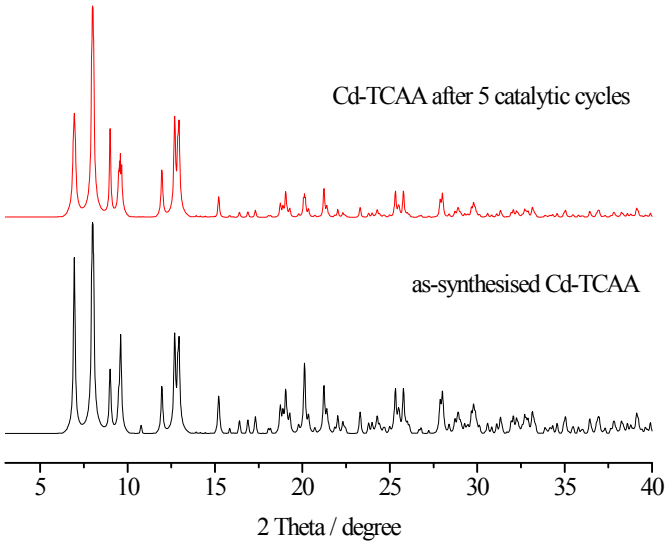

4.3 Figure S12 FT-IR spectra of Cd–TCAA (top) and Cd–TCAA after 5 cycles photodegradation of MB (bottom).

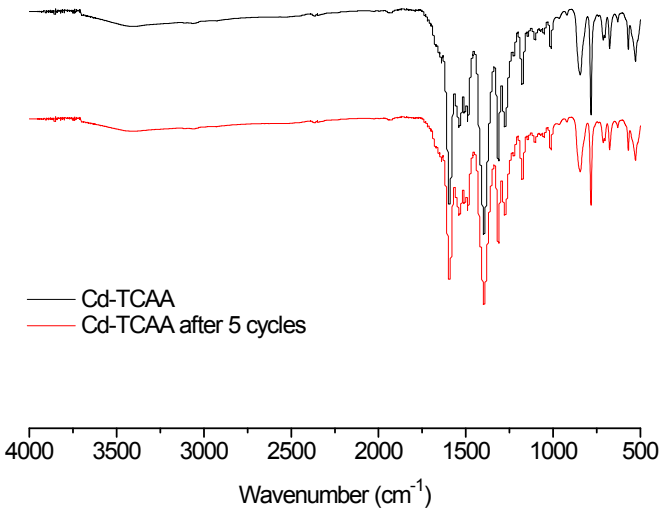

4.4 Table S2 The elemental analysis of the recovered Cd−TCAA after 5 cycles catalysis. (The C/H/N were performed on an Elementar Vario EL analyser, the Cd^{2+} contents were measured by Inductively Coupled Plasma Spectrometer (Perkin Elmer))

	C(%)	**H(%)**	**N(%)**	**Cd(mM)**
Original Cd−TCAA (theoretical)	49.17	2.54	6.62	0.79
Original Cd−TCAA (found)	49.18	2.55	6.60	0.78
Cd−TCAAafter 5 cycles	49.16	2.56	6.63	0.77
The solution after 5 cycles	-	-	-	n.d.

4.5 Table S3 Comparison of different MOF catalysts in the photodegradation of MB.

Entry	Catalyst	Time (min)	Removal (%)	Ref.
1	$[Co(L)(ADTZ)]\cdot H_2O$	180	87	[S2]
2	$[Cd(L)(ADTZ)(H_2O)]$	180	72	[S3]
3	$[Cu(3\text{-bpcb})_{0.5}(5\text{-AIP})]\cdot 2H_2O$	210	87	[S4]
4	$[Cu_2(L^2)_2(CrMo_6(OH)_5O_{19})(H_2O)_2]\cdot 2H_2O$	210	91	[S5]
5	$[(Zn(L)(mip)(H_2O))\cdot H_2O]_n$	150	56	[S6]
6	$(Me_2DABCO)_5(Cu_{15}Br_{24})Br$	150	92	[S7]
7	$Ni(C_{22}H_{26}N_2O_{10}S_2)\cdot 2CH_3OH$	140	95	[S8]
8	$[Ni_3(H_2L^2)2\cdot(HL^2)_2]\cdot(OH)_3\cdot(Ac)\cdot H_2O$	120	78	[S9]
9	$[(Pr_4N)(WS_4Cu_4(CN)_3)]_n$	180	94	[S10]
10	$[Co_{20}(OH)_{24}(MMT)_{12}(SO_4)](NO_3)_2\cdot 6H_2O$	180	83	[S11]
11	Cd-TCAA	175	81	This work

5. Reference

S1. J. Wang, C. He, P. Wu, J. Wang and C. Duan, *J. Am. Chem. Soc.*, 2011, **133**, 12402.

S2. X. Wang, C. Gong, Y. Qu, G. Liu and J. Zhang, *Chem. Res. Chin. Univ.*, 2014,**30**, 709.

S3. X.-L. Wang, Y. Qu, G.-C. Liu, J. Luan, H.-Y. Lin and X.-M. Kan, *Inorg. Chim. Acta*, 2014, **412**, 104.

S4. H. Lin, H. Lu, M. A. O. Le, J. Luan, X. Wang and G. Liu, *J. Chem. Sci.*, 2015,**127**, 1275.

S5. X. Wang, Z. Chang, H. Lin, A. Tian, G. Liu, J. Zhang and D. Liu, *RSC Adv.*, 2015, **5**, 14020.

S6. X. Wang, N. Chen, G. Liu, A. T. X. Sha and K. Ma, *Inorg. Chim. Acta*, 2015,**432**, 128.

S7. R. X. Yao, R. Hailili, X. Cui, L. Wang and X. M. Zhang, *Dalton Trans.*, 2015, **44**,3410.

S8. H. Wang, X. Meng, C. Fan, Y. Fan and C. Bi, *J. Mol. Struct.*, 2016, **1107**, 25.

S9. S. Y. Wei, J. L. Wang, C. S. Zhang, X.-T. Xu, X. X. Zhang, J. X. Wang and Y.-H. Xing, *ChemPlusChem*, 2015, **80**, 549.

S10. J. Zhang, C. Wang, Y. Wang, W. Chen, M. P. Cifuentes, M. G. Humphrey and C. Zhang, *J. Solid State Chem.*, 2015, **231**, 230.

S11. B. Mu and R.-D. Huang, *CrystEngComm*, 2016, **18**, 986.